MitoTEMPOL modulates mitophagy and histopathology of Wistar rat liver after streptozotocin injection

Rova Virgana [1, 2#], Julia Windi Gunadi [3#*], Nur Atik [4], Kwee Limdawati [5], Diana Krisanti Jasaputra [6], Roro Wahyudianingsih [7], Nadya Naurah Adrina Suardi [8], Ray Sebastian Soetadji [8], Hanna Goenawan [9, 10], Ronny Lesmana [9, 10], Arief Sjamsulaksan Kartasasmita [1, 2]

[1] Department of Ophthalmology, Universitas Padjadjaran, Bandung, West Java, Indonesia
[2] Cicendo National Eye Hospital, Bandung, West Java, Indonesia
[3] Department of Physiology, Faculty of Medicine, Maranatha Christian University, Bandung, West Java, Indonesia
[4] Biology Cell Division, Department of Biomedical Sciences, Faculty of Medicine, Universitas Padjadjaran, Bandung, West Java, Indonesia
[5] Department of Internal Medicine, Faculty of Medicine, Maranatha Christian University, Bandung, West Java, Indonesia
[6] Department of Pharmacology, Faculty of Medicine, Maranatha Christian University, Bandung, West Java, Indonesia
[7] Department of Pathology Anatomy, Faculty of Medicine, Maranatha Christian University, Bandung, West Java, Indonesia
[8] Faculty of Medicine, Maranatha Christian University, Bandung, West Java, Indonesia
[9] Physiology Division, Department of Biomedical Sciences, Faculty of Medicine, Universitas Padjadjaran, Bandung, West Java, Indonesia
[10] Physiology Molecular Laboratory, Biological Activity Division, Central Laboratory, Universitas Padjadjaran, Jatinangor, West Java, Indonesia

A B S T R A C T

Objective(s): This study aims to explore the effect of mitoTEMPOL on histopathology, lipid droplet, and mitophagy gene expression of Wistar rat's liver after injection of streptozotocin (STZ).

Materials and Methods: Twenty male Wistar rats were divided into 4 groups: Control (n=5); 100 mg/kg BW/day mitoTEMPOL orally (n=5); 50 mg/kg BW STZ intraperitoneal injection (n=5); and mitoTEMPOL+STZ (n=5). STZ was given a single dose, while mitoTEMPOL was given for 5 weeks after 1 week of STZ injection. Histopathological appearance, lipid droplets, mitophagy, and autophagy gene expression were examined after the mitoTEMPOL treatment.

Results: We found metabolic zone shifting that might be correlated with the liver activity of fatty acid oxidation in the STZ group, a decrease of lipid droplets in mitoTEMPOL and mitoTEMPOL + STZ compared with Control and STZ groups were found in this study. We also found significant changes in PINK1, Parkin, BNIP3, Mfn1, and LC3 gene expression, but no difference in Opa1, Fis1, Drp1, and p62 gene expression, suggesting a change of mitochondrial fusion rather than mitochondrial fission correlated with mitophagy.

Conclusion: All this concluded that mitoTEMPOL could act as a modulator of mitophagy and metabolic function of the liver, thus amplifying its crucial role in preventing mitochondrial damage in the liver in the early onset of diabetes mellitus.

Introduction

Diabetes mellitus is a serious disease that can cause complications in various organs of the body, thereby reducing the quality of life (1). Chronic hyperglycemia in diabetes causes glucotoxicity that might be correlated with mitochondrial dynamics (2). Glucotoxicity refers to excess carbohydrate intake in tissues that might be converted to triglycerides, free fatty acid, and free cholesterol, inducing steatosis in the liver (3). Recent studies have even shown that glucotoxicity can cause liver cell injury by inducing endoplasmic reticulum stress and hepatocyte cell death (3).

A chemical that is widely used for inducing diabetes type 1 and 2 in rodents is STZ (4-6). A single STZ injection causes partial destruction of the pancreas, providing a good model for the effect of glucotoxicity and lipotoxicity on mitochondrial oxidative dysfunction (4, 6). This single-dose STZ injection is less expensive and less time-consuming, compared with other models that induce diabetes (4). With its glucose moiety that is linked to β cells, STZ recognizes GLUT2 receptors in β cell plasma membranes, liver, and kidney (4, 7, 8). After injection, STZ is quickly metabolized by the liver and then excreted by the kidney, therefore its acute toxic effect on those organs could be neglected, then the effect of glucotoxicity on the liver could be extensively studied in this model (4, 9).

Although liver weight is only 2-4% of total body weight, it has a high oxygen consumption, approximately 60% of the organismal mitochondrial ATP demand is covered by hepatocytes (10, 11). Mitochondria in hepatocytes is participating in lipid and glucose production, storage, and consumption, free radicals production, cell survival, and death (12, 13). Chronic hyperglycemia was proven to be the contributing factor that increases ROS production in mitochondria (14, 15). Overproduction of ROS leads to oxidative stress where the balance of ROS and antioxidants in the cells is disturbed (14). This condition might lead to mitochondrial dysfunction characterized by reduced mitochondrial biogenesis, numbers, activities, and

altered membrane potential, further damaging other cell organelles, membranes, and proteins then finally inducing apoptosis (13, 16, 17). Therefore, maintaining homeostasis by recycling damaged organelles is needed to support mitochondrial dynamics, which is achieved by the work of autophagy, or more specifically mitochondrial autophagy (mitophagy) (17, 18).

Mitophagy is a process of maintaining homeostasis by eliminating damaged mitochondria (18). It could be induced through several pathways: PINK1/Parkin, BNIP/NIX, and FUNDC1, but the dominant pathway is PINK1/Parkin.(19-22) PINK1 is normally transported to the Inner Membrane Membrane (IMM) and then cleaved by the inner membrane protease PARL (Presenilins-associated rhomboid-like protein), but in mitochondrial dysfunction where there is a reduced membrane potential, PINK1 could not be transported into the IMM (22-24). This process makes the damaged mitochondria easily detected by autophagosomes, combined with Parkin recruitment that induces phosphorylation of Mfn1 and Mfn2 (22, 25, 26). PINK1/Parkin is activating mitophagy through indirect binding to autophagosomes, on the contrary, BNIP/NIX is activating mitophagy through indirect binding to autophagosomes (22, 25). These two pathways of mitophagy are induced by metabolic stress, oxidative stress, and fatty acid accumulation that eventually induced mitochondrial oxidative dysfunction (22, 25, 27).

Another way to improve mitochondrial oxidative dysfunction is by increasing antioxidants, especially mitochondria-targeted antioxidants (MTA). MTA could cross the mitochondrial phosphate bilayer and then eliminate excessive ROS at its central source (28). MitoTEMPOL is an MTA, derivative of TEMPOL (4-hydroxy-2,2,6,6-tetramethylpiperidine-1-oxy radical), which exhibits potent antioxidant properties. It contains the piperidine nitroxide (TEMPOL) and lipophilic cation triphenylphosphonium (TPP+) moiety. Tempol is a superoxide dismutase mimetic that dismutases superoxide in the catalytic cycle, whereas TPP is a membrane cation that accumulates several hundred-fold in the mitochondria because of the membrane potential. This combination creates mitochondrial targeting antioxidants that have effective superoxide scavenging abilities (29). Interestingly, MitoTEMPOL content has shown its ability to protect the liver from various injuries, such as liver-endotoxin injury, sepsis, hypertension, or colitis (30). Nevertheless, its molecular mechanism in the early stage of diabetes mellitus as a prevention strategy for complications in the liver is still unclear. This study aims to explore the effect of mitoTEMPOL on histopathology, lipid droplet, and mitophagy gene expression after the injection of single-dose STZ.

Materials and Methods
Animals
All animal protocols of the experiment were approved by the Research Ethics Committee of the Faculty of Medicine, Universitas Kristen Maranatha (No 165/KEP/VII/2021). Twenty 8-week old male Wistar rats weighing 210±20 g (n=5/group) were divided into 4 groups: 1) Control, 2) MitoTEMPOL 100 mg/kg BW/day orally, 3) STZ intraperitoneal injection 50 mg/kg BW, and 4) STZ intraperitoneal injection 50 mg/kg BW and MitoTEMPOL 10 mg/kg BW/day orally. Male Wistar rats were purchased

form Biofarma, Bandung, Indonesia. The rats were given a standard chow diet and were housed at room temperature with 12 hr of light and dark cycles every day. We conducted all procedures based on the use and care of laboratory guidelines.

MitoTEMPOL and STZ dose
MitoTEMPOL was purchased from Sigma-Aldrich Co. (Saint Louis, Missouri, USA), and STZ was purchased from Cayman Chemical Co. (Ann Arbor, Michigan, USA). We used a dose of MitoTEMPOL, 100 mg/kg BW for each rat, per os, 5 times a week, for 5 weeks while STZ in DMSO and sterile MilliQ was given via peritoneal injection, 50 mg/kg BW single dose. The dose of MitoTEMPOL and STZ was based on previous studies (4, 31). After 5 weeks, animals were euthanized (32), and the livers were rapidly excised and weighed. Then the livers were taken, and two sets of experiments were conducted, one for histopathological examination and the other for RNA extraction continued with semiquantitative PCR of mitophagy gene expression.

Hematoxylin and eosin (H&E staining)
For histopathological examination, the liver was fixed immediately in 10% formalin after extraction. The specimens were processed for paraffin embedding followed by the preparation of 2-μm thick sections. The sections were stained with hematoxylin and eosin (H&E) for light microscope examination (LEICA ICC50, Wetzlar, Germany) with 100x and 400x magnification. Images were captured using Leica Application Suite (LEICA, Wetzlar, Germany). Images were analyzed by an expert pathologist. We evaluated the histopathological changes using a scoring system that had been used in our previous study (33). The evaluation of the livers was divided into three categories: congestion/sinusoidal dilatation, cloudy swelling/injury, and inflammation. For scoring of liver congestion or sinusoidal dilatation score, sections were assessed based on liver zones, using this following scoring: 0=No congestion/sinusoidal dilatation; 1=Mild congestion or centrilobular (zone III) sinusoidal dilatation; 2=Moderate congestion or centrilobular (zone II) sinusoidal dilatation; and 3=Severe congestion or centrilobular (zone I) sinusoidal dilatation. For scoring of cloudy swelling/hepatic injury, we used the following scoring: 0=No cloudy swelling/hepatic injury; 1=Mild cloudy swelling/hepatic injury (zone III); 2=Moderate cloudy swelling/hepatic injury (zone II); 3=Severe cloudy swelling/hepatic injury (zone I). For scoring the inflammation severity, we used the following scoring: 0=No hepatic inflammation; 1=Mild hepatic inflammation or periportal inflammation; 2=Moderate hepatic inflammation or periportal and intraparenchymal inflammation; and 3=Severe hepatic inflammation or periportal and intraparenchymal inflammation with bridging necrosis (33).

Oil red O staining
For lipid droplet quantification, we used oil red O staining. The oil red O was purchased from Sigma Aldrich Co. (Saint Louis, Missouri, USA). We used 0.5-gram oil red O dissolved in 100 ml isopropanol to make the oil red O stock stain, then we diluted 30 ml of the stock stain with 20 ml of distilled water to make the oil red O working solution. The specimens were processed for paraffin embedding

Table 1. Primers used for semi quantitative-PCR analysis of mitophagy and autophagy gene expression

Gene symbol	Primer sequence (5' to 3') Upper strand: sense Lower strand: antisense	Product size (bp)	References
PINK1	TGCAATGCCGCTGTGTATGA TCTGCTCCCTTTGAGACGAC	113	(35)
Parkin	CCAAACCGGATGAGTGGTGAGTGC ACACGGCAGGGAGTAGCCAAGTTG	303	(36)
BNIP3	GAAGCGCACAGCTACTCTCA TCCAATGTAGATCCCCAAGCC	142	(37)
Mfn1	TGACTTGGACTACTCGTGCG GTGGCCATTTCTTGCTGGAC	133	(35)
Mfn2	TCAGTAGCCAATCTGGACCT TCTCTTGGATGTAGGCCCCC	277	(35)
Opa1	ATCATCTGCCACGGGTTGTT GAGAGCGCGTCATCATCTCA	120	(38)
Fis1	AAAGAGGAGCAGCGGGATTA TGGGGCTCAGTCTGTAACAG	110	(39)
Drp1	CGCTGATCCCGGTCATCAAT ACTCCATTTTCTTCTCCTGTTGT	247	(35)
LC3	GGTCCAGTTGTGCCTTTATTGA GTGTGTGGGTTGTGTACGTCG	153	(40)
p62	CTAGGCATCGAGGTTGACATT CTTGGCTGAGTACCACTCTTATC	116	(41)
GAPDH	GTTACCAGGGCTGCCTTCTC GATGGTGATGGGTTTCCCGT	177	(42)

followed by the preparation of 2-μm thick sections. After deparaffinization, xylene and ethanol were used to rehydrate the slides, then we stained them with freshly prepared oil-red O working solutions for 15 min. The slides were then rinsed with 60% isopropanol, continued with 4 min of light staining with hematoxylin, then rinsing with distilled water. We mounted the slides with Entellan from Marck & Co. (Kenilworth, New Jersey, United States). Images of the slides were captured using Leica Application Suite (LEICA, Wetzlar, Germany). A total of lipid droplets from each slide was quantified using Image J, 10 fields from each sample, then averaged (33).

Total RNA extractions and semi-quantitative PCR

The total RNA of the liver of male Wistar rats was extracted using TRIsure reagent (Bioline, London, United Kingdom) according to the manufacturer's instructions. Purity and concentrations of RNA were assessed using spectrophotometry analysis, at 268/280 nm absorbance (Multiscan Go, Thermo Fisher Scientific, Massachusetts, United States). Semi-quantitative PCR was performed

using The One-Step RT PCR Kit (Bioline, London, United Kingdom). The housekeeping gene GAPDH was measured for each sample as an internal control and normalization. Gel electrophoresis was performed using Mupid Exu Submarine Electrophoresis System (Mupid Co., Tokyo, Japan), while visualization of the gels was conducted using BluPAD Dual LED Blue/White Light Transilluminator (Bio-Helix Co., Taiwan). For quantification of the PCR bands using Image J (34). The list of primer sequences was provided in Table 1.

Statistical analysis

All data obtained in this study were presented as mean±SEM. The results were analyzed using the Kruskal Wallis one-Way analysis of variance test, followed by LSD/Mann Whitney for the *post hoc* test. Statistical analysis was performed using SPSS software 20.0. The level significance test was fixed at $P<0.05$.
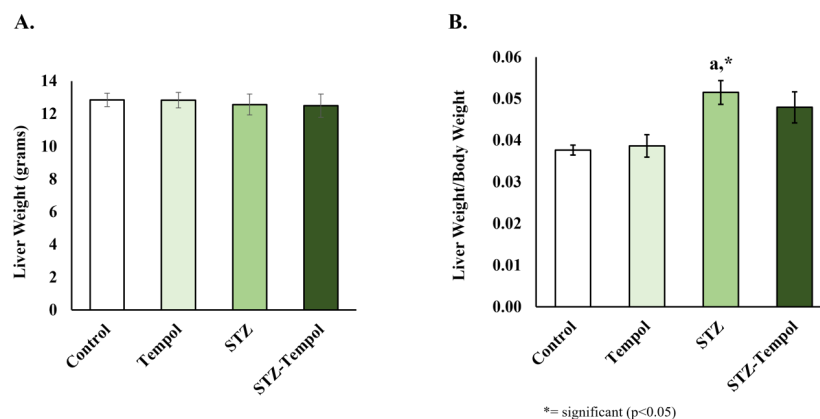
Results

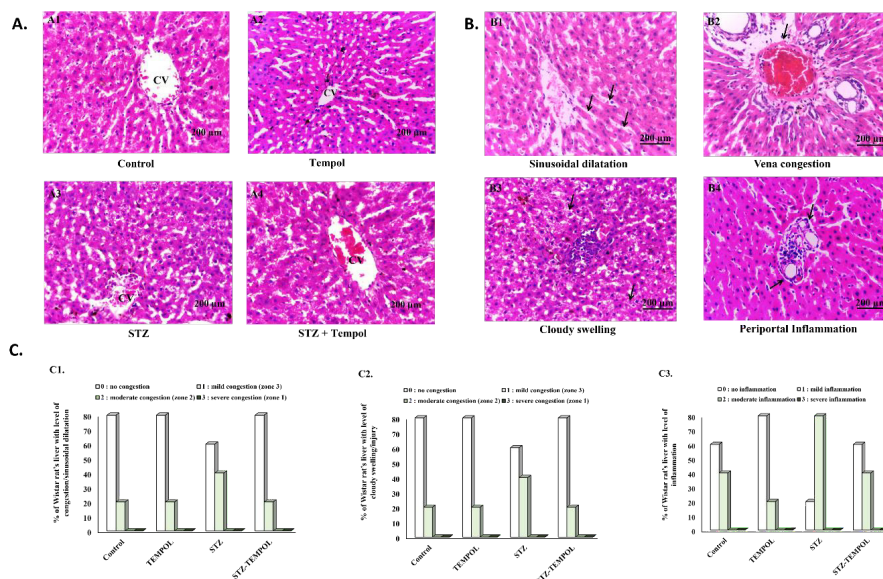*STZ Injection increased liver weight/body weight ratio*

As shown in Figure 1, STZ injection did not influence liver weight (Figure 1A) but increased liver weight/body weight (Figure 1B). The significant increase in liver weight/body weight ratio between control and STZ ($P=0.0385$) was the result of decreased body weight induced by STZ injection, but no significant changes were found in other groups (Figure 1B).

Effect of MitoTEMPOL on histopathological appearance after STZ injection

We examined the histopathological appearance of the liver based on the scoring system applied in our previous study (33). The general histopathological appearance of all groups was presented in Figure 2A (A1=control, A2=TEMPOL, A3=STZ, A4=STZ-TEMPOL), while the representative figure of each scoring system (B1 and B2=congestion/ sinusoidal dilatation, B3=cloudy swelling/injury, B4=inflammation) was presented in Figure 2B, and graphical result to show the percentages of samples for each scoring was shown in Figure 2C. For congestion/sinusoidal dilatation, we found 80% samples with level 0 and 20% samples with level 1 in control, TEMPOL, and STZ-TEMPOL groups; but we found 60% samples with level 0 and 40% samples with level 1 in the STZ group (Figure 2C-1). For cloudy swelling/injury, we found 100% samples with

Figure 1. STZ injection increased liver/body weight ratio in rats. (A) No difference in liver weight between any groups. (B) Liver weight/body weight ratio increased in streptozotocin (STZ) groups compared with the control (a; *P*<0.05), but no significant differences were found in other groups Tempol: MitoTEMPOL group; STZ: Streptozotocin group; STZ-Tempol: Streptozotocin+MitoTEMPOL group
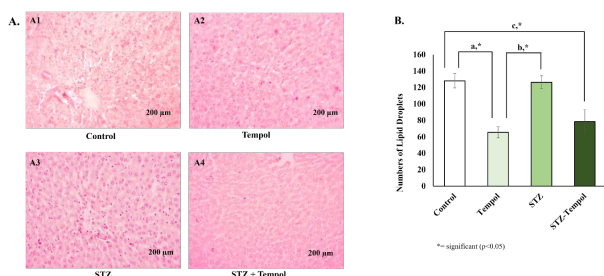
Figure 2. General appearance and scoring of liver histopathology after streptozotocin (STZ) injection and MitoTEMPOL ingestion (A) General appearance of liver histopathology of all groups (A1=Control, A2=TEMPOL, A3=STZ, and A4=STZ-TEMPOL). (B) Representative figures of each liver histopathology scoring (B1=Sinusoidal dilatation, B2=Vena congestion, B3=Clouding swelling, and B4=periportal inflammation). (C) Percentage of Wistar rat liver for each histopathology scoring (C1=Congestion/sinusoidal dilatation, C2=Cloudy swelling/injury, and C3=Inflammation). No significant differences in liver histopathology scoring were found between any groups
Tempol: MitoTEMPOL group; STZ: Streptozotocin group; STZ-Tempol: Streptozotocin+MitoTEMPOL group

level 0 in the control and TEMPOL groups, 60% samples with level 0 and 40% samples with level 1 in the STZ group, and 80% samples with level 0 and 20% samples in level 1 in STZ-TEMPOL group (Figure 2C-2). For inflammation, we found 60% samples with level 0, 40% samples with level 1 in control and STZ-TEMPOL groups, 80% samples with level 0, and 20% samples with level 1 in the TEMPOL group, 20% samples with level 0, and 80% samples with level 1 in the STZ group (Figure 2C-3).

Effect of MitoTEMPOL on number of lipid droplets after STZ injection

The effect of MitoTEMPOL on a number of lipid droplets was presented in Figure 3. Figure 3A showed a representative figure of each group (Control, TEMPOL, STZ, and STZ-TEMPOL), while Figure 3B presented a graphical result for quantification of lipid droplets in each group, and we found a significant decrease of lipid droplets in Tempol and STZ-TEMPOL groups compared with control and STZ groups ($P<0.05$).
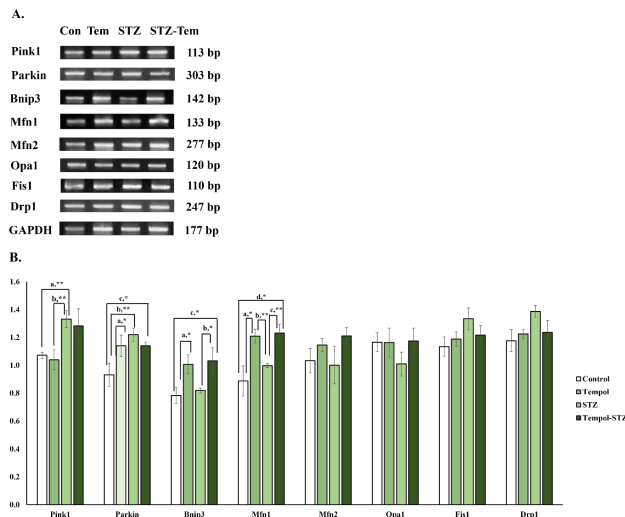

Figure 3. Oil red O staining of Wistar rat liver after streptozotocin (STZ) injection and MitoTEMPOL ingestion (A) Representative Figures of Oil Red O Staining from each group of the experiment (A1=Control, A2=TEMPOL, A3=STZ, and A4=STZ-TEMPOL) (B) Graphical result of numbers of lipid droplet quantification from each group of experiment. There were significant differences ($P<0.05$) between control and TEMPOL (a), TEMPOL and STZ, and between Control and STZ-TEMPOL (b)
Tempol: MitoTEMPOL group; STZ: Streptozotocin group; STZ-Tempol: Streptozotocin+MitoTEMPOL group

Effect of MitoTEMPOL on mitophagy gene expression after STZ injection

We presented the bands of mitophagy gene expression (Pink1, Parkin, BNIP3, Mfn1, Mfn2, and Drp1) in Figure 4A, and the graphical result of mitophagy gene expression in Figure 4B. We found a very significant increase in PINK1 gene expression in the STZ group compared with the control (1.24-fold, $P=0.009$) and TEMPOL group (1.28-fold, $P=0.009$). We also found a significant increase in Parkin gene expression in the TEMPOL group (1.22-fold, $P=0.033$), STZ group (1.31-fold, $P=0.005$), and STZ-TEMPOL group (1.22-fold, $P=0.034$) compared with Control. For BNIP3 gene expression, we found a significant increase in the TEMPOL group compared with the control (1.28-fold, $P=0.029$), and in the STZ-TEMPOL group compared with STZ (1.26-fold, $P=0.036$) and control (1.32-fold, $P=0.016$). For Mfn1 gene expression, we found a significant increase in the TEMPOL group compared with the control (1.36-fold, $P=0.028$) and STZ group (1.21-fold, $P=0.009$); and between the STZ-TEMPOL group with STZ (1.26-fold, $P=0.009$) and control (1.23-fold, $P=0.028$). But we found no difference in Opa1 ($P=0.515$), Fis1 ($P=0.227$), and Drp1 ($P=0.115$) gene expression between any groups, as shown in Figures 4A and 4B.

Effect of MitoTEMPOL on autophagy gene expression after STZ injection

We presented the bands of autophagy gene expression (LC3 and p62) in Figure 5A and the graphical result of autophagy gene expression in Figure 5B. We found no significant difference between any groups, but interestingly we found a significant increase of LC3 gene expression in the TEMPOL group compared with the control (1.26-fold, $P=0.027$) and STZ groups (1.29-fold, $P=0.018$), and in STZ-TEMPOL compared with STZ group (1.24 fold, $P=0.044$). No significant differences were found in p62 gene expression ($P=0.293$), but there is a tendency for a decrease in p62 gene expression in TEMPOL and STZ-TEMPOL groups compared with control and STZ groups.
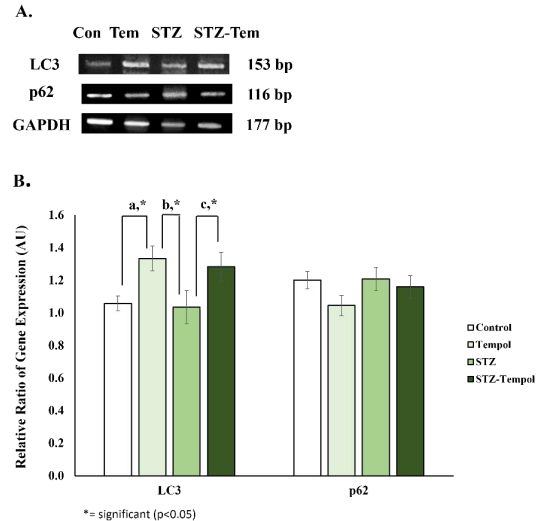
Figure 4. Effect of MitoTEMPOL on mitophagy gene expression after streptozotocin (STZ) injection in rat. (A) PCR bands of mitophagy gene expression after STZ injection and MitoTEMPOL ingestion. (B) Significant increase in Pink1, Parkin gene expression was found in the STZ group compared with control, but we found a decrease of BNIP3 and Mfn1 in STZ group compared with control and TEMPOL groups. But we found no significant differences in Mfn2, Opa1, Fis1, and Drp1 gene expression between any groups
Tempol: MitoTEMPOL group; STZ: Streptozotocin group; STZ-Tempol: Streptozotocin+MitoTEMPOL group; Pink1: PTEN-induced kinase 1; Parkin: Parkin RBR E3 ubiquitin-protein ligase; Bnip3: Bcl2/adenovirus E1B 19-kDa interacting protein 3; Mfn1: Mitofusin-1; Mfn3, Mitofusin-2; Opa1: Optic atrophy 1; Fis1: Mitochondrial fission 1 protein; Drp1: Dynamin-related protein 1

Discussion

STZ-induced diabetes in the rat model is one of the most common models to mimic acute and chronic complications of diabetes and the potential therapy to treat diabetes (4, 43). β cell destruction started 3 days after STZ administration, and reaches the peak of destruction after 2-4 weeks in rats, reducing β active cells that lead to a diabetic state (44, 45). In this study, we found a decrease in body weight in STZ and STZ-Tempol groups, compared with control and tempol groups (Figure 1A), and a significant increase in liver weight/body weight ratio between STZ and control (Figure 1C), whereas the liver weight of any group was not significantly different (Figure 1B). This condition might result from the injection of STZ which causes insulin decrease, inducing utilization of other energy sources that finally leads to weight loss (4,46). STZ injection was also reported to induce liver tumors in laboratory animals (47), but in this study, we found no difference in liver weight in any group, which means the increase in liver weight/body weight ratio was ultimately because of the decreased body weight.

In this study, we also examined the liver histopathology scoring between all groups. The scoring was defined based on our previous study that correlated the metabolic zonation (Zones I, II, and III) with liver histopathology (congestion/sinusoidal dilatation, cloudy swelling/injury, inflammation) and autophagy (33, 48). For congestion/sinusoidal dilatation, we found an increase of samples with level 1 in the STZ group (40%) compared with samples with level 1 in control, TEMPOL, and STZ-TEMPOL groups (20%), as shown in Figure 2C-1. For cloudy swelling/injury, we also found an increase of samples with level 1 in the STZ group (40%) compared with control and TEMPOL groups (0%)

Figure 5. Effect of MitoTEMPOL on autophagy gene expression after streptozotocin (STZ) injection in rat. (A) PCR bands of autophagy gene expression after STZ injection and Mitotempol ingestion (B) A significant difference in LC3 gene expression was found in TEMPOL compared with control and STZ, and between STZ-TEMPOL and STZ, but no difference in p62 gene expression in any groups
Tempol: MitoTEMPOL group; STZ: Streptozotocin group; STZ-Tempol: Streptozotocin+MitoTEMPOL group; LC3: Microtubule-associated protein 1A/1B-light chain 3; Sequestosome-1

and STZ-TEMPOL group (20%), as shown in Figure 2C-2. For inflammation, we found an increase of samples with level 1 in the STZ group (80%), compared with samples in the control and STZ-TEMPOL groups (40%) and samples with level 1 in the TEMPOL group (20%), as shown in Figure 2C-3. The increased level 1 of congestion/sinusoidal dilatation, cloudy swelling/injury, and inflammation in the STZ group might have resulted from the injury induced by STZ injection and might also be correlated with shifting of active metabolic zonation. We hypothesized that MitoTEMPOL might improve the histopathology appearance because of its role as a potent antioxidant (30, 49).

MitoTEMPOL also has been proven to have a protective role against NAFLD (Non-Alcoholic Fatty Liver Disease) by reducing lipid droplets in HFD-induced obese mice and inhibit foam cell formation to prevent atherosclerosis (50, 51). Recent studies have confirmed that the contact sites between lipid droplets and endoplasmic reticulum in mitochondria have a critical role in the cell metabolism of lipids. These contact sites are important for inter-organelle communication to maintain body homeostasis. In hepatocytes, the breakdown of this communication might induce lipid droplet accumulation as an early sign of NAFLD. In this study, we did not induce a high-fat diet for the experiment animals, and this might explain why the STZ group has a similar number of lipid droplets as the control group. Interestingly, we found a significant decrease of lipid droplets in the TEMPOL and STZ-TEMPOL groups (Figure 3) that might have a protective role in NAFLD prevention that might occur as a chronic complication of diabetes.

Experimental animals induced by STZ are a useful model to determine the effect of beta-cell glucotoxicity in diabetes mellitus (52). Literature studies show that induction of experimental animals with single-dose STZ is a suitable model to study the mechanism of changes in mitochondrial structure and function that occur due to beta-cell glucotoxicity causing mitochondrial dysfunction (53).

One of the things that cause mitochondrial dysfunction is the inhibition of mitophagy, which can be seen from the expression of PINK1, Parkin, and BNIP3 genes (54).

In this study, we found a significant increase of PINK1 and Parkin in STZ groups which might indicate an increase in mitochondrial fission, while BNIP3 gene expression and Mfn1 were decreased in STZ which might be correlated with mitochondrial fusion (Figure 4). This result showed an alteration of mitophagy gene expression in Wistar rat livers after STZ injection and in MitoTEMPOL ingestion compared with STZ and control groups. There are 3 pathways of mitophagy: PINK1/Parkin, BNIP/NIX, and FUNDC1, with PINK1/Parkin as a major pathway. The mitochondria life cycle reveals the interaction between mitochondrial fusion (Mfn1, Mfn2, and Opa1), mitochondrial fission (Fis1 and Drp1), and mitophagy (PINK1, Parkin, BNIP3, etc). Where mitochondrial fusion prevents the removal of mitochondria, fission produces impaired mitochondria as a target of autophagy (55). Mfn1 and Mfn2 mediate mitochondrial outer membrane fusion in mammals, while Opa1 mediates mitochondrial inner membrane fusion. Drp1 mediates mitochondrial fission that cycles between cytosol and the mitochondrial outer membrane (56). Increase of Mfn1 and Mfn2 showed an increase in mitochondrial outer membrane fusion, while the increase of PINK1, Parkin, and Drp1 showed activated mitochondrial fission.

Mitochondrial fragmentation due to fission/fusion imbalance has often been linked to mitochondrial dysfunction and apoptosis in diabetes Mellitus (57). Mitochondrial fission and fusion balance is required for appropriate mitochondrial functions. These processes are important because of their role in maintaining mitochondrial DNA, segregating damaged mitochondria by mitophagy, distributing and moving mitochondria within the cell, and also for mitochondrial morphology regulation (58, 59). Induction of fusion and inhibition of fission by mitotempol might be correlated with its effect to maintain mitochondrial dynamics that might be disturbed because of STZ injection. The role of mitoTEMPOL to maintain homeostasis was also shown by the significant increase of LC3 gene expression in TEMPOL and STZ-TEMPOL groups, whereas in the STZ group, we found a decrease of LC3 and an increase of p62 (Figure 5). These results showed that autophagy might be activated after MitoTEMPOL ingestion, whereas STZ injection might inhibit autophagy, but further study should be conducted to support this hypothesis.

Conclusion

STZ injection in rats is a common model to mimic diabetes, and the purpose of this model is to evaluate the mechanism of MitoTEMPOL as a potent antioxidant for preventing complications of diabetes in the early stages. With its ability to prevent oxidative stress, which induces mitochondrial dysfunction in diabetes, the effect of mitoTEMPOL on Wistar rat liver induced by STZ injection is important to understand its mechanism in preventing acute and chronic complications of diabetes. MitoTEMPOL improves body weight, as seen in the increase of liver weight/body weight ratio, changes histopathology appearance, lipid droplets, and mitophagy gene expression after 5 weeks of STZ injection. In conclusion, mitoTEMPOL has an important role as a potent mitochondrial-targeted antioxidant to prevent complications of diabetes, especially with its correlation to mitophagy which might be correlated with histopathology improvement and reduced lipid droplets in the liver.

Authors' Contributions

RV, RL, and JWG designed the experiments; NN, RS, and DKJ performed experiments and collected data; RW, NA, and RL discussed the results and interpretation, JWG and HG drafted the manuscript; KL, RV, RL, and ASK supervised and managed the study; all of the authors approved the final manuscript.

Conflicts of Interest

The authors declared no conflicts of interest.

References

1. Papatheodorou K, Banach M, Bekiari E, Rizzo M, Edmonds M. Complications of diabetes 2017. J Diabetes Res 2018; 2018: 3086167.
2. Kobayashi S, Zhao F, Zhang Z, Kobayashi T, Huang Y, Shi B, *et al*. Mitochondrial fission and mitophagy coordinately restrict high glucose toxicity in cardiomyocytes. Front Physiol 2020; 11: 604069.
3. Mota M, Banini BA, Cazanave SC, Sanyal AJ. Molecular mechanisms of lipotoxicity and glucotoxicity in nonalcoholic fatty liver disease. Metabolism 2016; 65: 1049–1061.
4. Wu J, Yan L-J. Streptozotocin-induced type 1 diabetes in rodents as a model for studying mitochondrial mechanisms of diabetic β cell glucotoxicity. Diabetes Metab Syndr Obes 2015; 8: 181-188.
5. Ghasemi A, Khalifi S, Jedi S. Streptozotocin-nicotinamide-induced rat model of type 2 diabetes (review). Acta Physiol Hung 2014; 101: 408–420.
6. Deeds MC, Anderson JM, Armstrong AS, Gastineau DA, Hiddinga HJ, Jahangir A, *et al*. Single dose streptozotocin-induced diabetes: considerations for study design in islet transplantation models. Lab Anim 2011; 45: 131-140.
7. Johansson EB, Tjalve H. Studies on the tissue-disposition and fate of [14C]streptozotocin with special reference to the pancreatic islets. Acta Endocrinol (Copenh) 1978; 89: 339–351.
8. Lenzen S. The mechanisms of alloxan- and streptozotocin-induced diabetes. Diabetologia 2008; 51: 216–226.
9. Tesch GH, Allen TJ. Rodent models of streptozotocin-induced diabetic nephropathy. Nephrology (Carlton) 2007; 12: 261–266.
10. Rolfe DF, Brown GC. Cellular energy utilization and molecular origin of standard metabolic rate in mammals. Physiol Rev 1997; 77: 731–758.
11. Shum M, Ngo J, Shirihai OS, Liesa M. Mitochondrial oxidative function in NAFLD: Friend or foe? Mol Metab 2021; 50: 101134.
12. Kim J-A, Wei Y, Sowers JR. Role of mitochondrial dysfunction in insulin resistance. Circ Res. 2008; 102: 401-414.
13. Bhatti JS, Bhatti GK, Reddy PH. Mitochondrial dysfunction and oxidative stress in metabolic disorders-A step towards mitochondria based therapeutic strategies. Biochim Biophys acta Mol basis Dis 2017; 1863: 1066–1077.
14. Yan L-J. Pathogenesis of chronic hyperglycemia: From reductive stress to oxidative stress. J Diabetes Res 2014; 2014: 137919.
15. Giri B, Dey S, Das T, Sarkar M, Banerjee J, Dash SK. Chronic hyperglycemia mediated physiological alteration and metabolic distortion leads to organ dysfunction, infection, cancer progression and other pathophysiological consequences: An update on glucose toxicity. Biomed Pharmacother 2018; 107: 306-228.
16. Pieczenik SR, Neustadt J. Mitochondrial dysfunction and

molecular pathways of disease. Exp Mol Pathol 2007; 83: 84-92.

17. Belousov DM, Mikhaylenko E V, Somasundaram SG, Kirkland CE, Aliev G. The dawn of mitophagy: What do we know by now? Curr Neuropharmacol 2021; 19: 170-192.

18. Pickles S, Vigié P, Youle RJ. Mitophagy and quality control mechanisms in mitochondrial maintenance. Curr Biol 2018; 28: 170–185.

19. Yuan Y, Zheng Y, Zhang X, Chen Y, Wu X, Wu J, *et al*. BNIP3L/NIX-mediated mitophagy protects against ischemic brain injury independent of PARK2. Autophagy 2017; 13: 1754–1766.

20. Li Y, Liu Z, Zhang Y, Zhao Q, Wang X, Lu P, *et al*. PEDF protects cardiomyocytes by promoting FUNDC1-mediated mitophagy via PEDF-R under hypoxic condition. Int J Mol Med 2018; 41: 3394-3404.

21. Sato S, Furuya N. Induction of PINK1/Parkin-Mediated Mitophagy. Methods Mol Biol 2018; 1759: 9–17.

22. Su Z, Nie Y, Huang X, Zhu Y, Feng B, Tang L, *et al*. Mitophagy in hepatic insulin resistance: Therapeutic potential and concerns. Front Pharmacol 2019; 10: 1193.

23. Lemasters JJ, Zhong Z. Mitophagy in hepatocytes: Types, initiators and role in adaptive ethanol metabolism. Liver Res 2018; 2: 125–132.

24. Wang H, Ni H-M, Chao X, Ma X, Rodriguez YA, Chavan H, *et al*. Double deletion of PINK1 and Parkin impairs hepatic mitophagy and exacerbates acetaminophen-induced liver injury in mice. Redox Biol 2019; 22: 101148.

25. Moreira OC, Estébanez B, Martínez-Florez S, de Paz JA, Cuevas MJ, González-Gallego J. Mitochondrial function and mitophagy in the elderly: Effects of exercise. Oxid Med Cell Longev 2017; 2017: 2012798.

26. Eid N, Ito Y, Otsuki Y. Triggering of parkin mitochondrial translocation in mitophagy: Implications for liver diseases. Front Pharmacol 2016; 7: 100.

27. Glick D, Zhang W, Beaton M, Marsboom G, Gruber M, Simon MC, *et al*. BNip3 regulates mitochondrial function and lipid metabolism in the liver. Mol Cell Biol 2012; 32: 2570–2584.

28. Oyewole AO, Birch-Machin MA. Mitochondria-targeted antioxidants. FASEB J 2015; 29: 4766–4671.

29. Cohen SD, Pumford NR, Khairallah EA, Boekelheide K, Pohl LR, Amouzadeh HR, *et al*. Selective protein covalent binding and target organ toxicity. Toxicol Appl Pharmacol 1997; 143: 1–12.

30. Du K, Farhood A, Jaeschke H. Mitochondria-targeted antioxidant Mito-Tempo protects against acetaminophen hepatotoxicity. Arch Toxicol 2017; 91: 761–773.

31. Ahmed LA, Shehata NI, Abdelkader NF, Khattab MM. Tempol, a superoxide dismutase mimetic agent, ameliorates cisplatin-induced nephrotoxicity through alleviation of mitochondrial dysfunction in mice. PLoS One 2014; 9: e108889.

32. Dey S, DeMazumder D, Sidor A, Foster DB, O'Rourke B. Mitochondrial ROS drive sudden cardiac death and chronic proteome remodeling in heart failure. Circ Res 2018;123:356-371.

33. Gunadi JW, Tarawan VM, Daniel Ray HR, Wahyudianingsih R, Lucretia T, Tanuwijaya F, *et al*. Different training intensities induced autophagy and histopathology appearances potentially associated with lipid metabolism in wistar rat liver. Heliyon 2020; 6: e03874.

34. Tarawan VM, Gunadi JW, Setiawan, Lesmana R, Goenawan H, Meilina DE, *et al*. Alteration of autophagy gene expression by different intensity of exercise in gastrocnemius and soleus muscles of wistar rats. J Sports Sci Med 2019; 18: 146-154.

35. Lesmana R, Budi Prasetyo W, Ray HRD, Tarawan V, Goenawan H, Setiawan I, *et al*. Exercise serum alters genes related mitochondria in cardiomyocyte culture cell. J Pendidik Jasm dan Olahraga 2020; 5: 102-110.

36. Maurya SK, Herrera JL, Sahoo SK, Reis FCG, Vega RB, Kelly DP, *et al*. Sarcolipin signaling promotes mitochondrial biogenesis and oxidative metabolism in skeletal muscle. Cell Rep 2018; 24: 2919-2931.

37. Montagna C, Di Giacomo G, Rizza S, Cardaci S, Ferraro E, Grumati P, *et al*. S-nitrosoglutathione reductase deficiency-induced S-nitrosylation results in neuromuscular dysfunction. Antioxid Redox Signal 2014; 21: 570-587.

38. Hong JY, Kim H, Lee J, Jeon W-J, Baek SH, Ha I-H. Neurotherapeutic Effect of *Inula britannica* var. chinensis against H(2)O(2)-induced oxidative stress and mitochondrial dysfunction in cortical neurons. Antioxidants 2021; 10: 375.

39. Abdullaev S, Gubina N, Bulanova T, Gaziev A. Assessment of nuclear and mitochondrial DNA, expression of mitochondria-related genes in different brain regions in rats after whole-body X-ray irradiation. Int J Mol Sci 2020; 21: 1196.

40. Yin P, Wan C, He S, Xu X, Liu M, Song S, *et al*. Transport stress causes damage in rats' liver and triggers liver autophagy. Biotechnol An Indian J 2013; 8: 1561-1566.

41. Kowalik MA, Perra A, Ledda-Columbano GM, Ippolito G, Piacentini M, Columbano A, *et al*. Induction of autophagy promotes the growth of early preneoplastic rat liver nodules. Oncotarget 2016; 7: 5788-5799.

42. Wang K, Wang F, Bao J-P, Xie Z-Y, Chen L, Zhou B-Y, *et al*. Tumor necrosis factor α modulates sodium-activated potassium channel SLICK in rat dorsal horn neurons via p38 MAPK activation pathway. J Pain Res 2017; 10: 1265-1271.

43. Eleazu CO, Iroaganachi M, Okafor PN, Ijeh II, Eleazu KC. Ameliorative potentials of ginger (*Zingiber officinale* Roscoe) on relative organ weights in streptozotocin induced diabetic rats. Int J Biomed Sci 2013; 9: 82-90.

44. Eleazu CO, Iroaganachi M, Eleazu KC. Ameliorative potentials of cocoyam (*Colocasia esculenta* L.) and unripe plantain (*Musa paradisiaca* L.) on the relative tissue weights of streptozotocin-induced diabetic rats. J Diabetes Res 2013; 2013: 160964.

45. Adeghate E, Ponery AS. GABA in the endocrine pancreas: cellular localization and function in normal and diabetic rats. Tissue Cell 2002; 34: 1–6.

46. Ho J, Tseng C-Y, Ma W-H, Ong W-K, Chen Y-F, Chen M-H, *et al*. Multiple intravenous transplantations of mesenchymal stem cells effectively restore long-term blood glucose homeostasis by hepatic engraftment and β-Cell differentiation in streptozocin-induced diabetic mice. Cell Transplant 2011; 21: 997-1009.

47. Vivek KS. Streptozotocin: An experimental tool in diabetes and alzheimer's disease: A review. Int J Pharma Res Dev 2010;2:1-7.

48. Trefts E, Gannon M, Wasserman DH. The liver. Curr Biol 2017; 27: 1147–1151.

49. Trnka J, Blaikie F, Logan A, Smith R, Murphy M. Antioxidant properties of MitoTEMPOL and its hydroxylamine. Free Radic Res 2009; 43: 4–12.

50. Wu J, Zheng L, Mo J, Yao X, Fan C, Bao Y. Protective effects of MitoTEMPO on nonalcoholic fatty liver disease via regulating myeloid-derived suppressor cells and inflammation in mice. Biomed Res Int 2020; 2020: 9329427.

51. Ma Y, Huang Z, Zhou Z, He X, Wang Y, Meng C, *et al*. A novel antioxidant Mito-Tempol inhibits ox-LDL-induced foam cell formation through restoration of autophagy flux. Free Radic Biol Med 2018; 129: 463–472.

52. Guven A, Yavuz O, Cam M, Ercan F, Bukan N, Comunoglu C, *et al*. Effects of melatonin on streptozotocin-induced diabetic liver injury in rats. Acta Histochem 2006;108:85–93.

53. Sivitz WI, Yorek MA. Mitochondrial dysfunction in diabetes: from molecular mechanisms to functional significance and therapeutic opportunities. Antioxid Redox Signal 2010; 12: 537–77.

54. Durcan TM, Fon EA. The three 'P's of mitophagy: PARKIN, PINK1, and post-translational modifications. Genes Dev 2015; 29: 989-999.

55. Twig G, Shirihai OS. The interplay between mitochondrial dynamics and mitophagy. Antioxid Redox Signal 2011; 14: 1939-1951.

56. Van der Bliek AM, Shen Q, Kawajiri S. Mechanisms of mitochondrial fission and fusion. Cold Spring Harb Perspect Biol 2013; 5: a011072.

57. Williams M, Caino MC. Mitochondrial dynamics in type 2 diabetes and cancer. Front Endocrinol 2018; 9: 211.

58. Bereiter-Hahn J, Vöth M. Dynamics of mitochondria in living cells: Shape changes, dislocations, fusion, and fission of mitochondria. Microsc Res Tech 1994; 27: 198-219.

59. Amiri M, Hollenbeck PJ. Mitochondrial biogenesis in the axons of vertebrate peripheral neurons. Dev Neurobiol 2008; 68: 1348-1361.